

Document downloaded from:

<http://hdl.handle.net/10251/59124>

This paper must be cited as:

Benajes Calvo, J.V.; Novella Rosa, R.; García Martínez, A.; Arthozoul ., SJL. (2011). The role of in-cylinder gas density and oxygen concentration on late spray mixing and soot oxidation processes. *Energy*. 36:1599-1611. doi:10.1016/j.energy.2010.12.071.



The final publication is available at

<http://dx.doi.org/10.1016/j.energy.2010.12.071>

Copyright Elsevier

Additional Information

The Role of In-Cylinder Gas Density and Oxygen Concentration on Late Spray Mixing and Soot Oxidation Processes

Jesús Benajes, Ricardo Novella, Antonio García and Simon Arthozoul*

CMT-Motores Térmicos

Universidad Politécnica de Valencia

Camino de Vera s/n, 46022, Valencia (Spain)

(*) Corresponding author: Ricardo Novella, E-Mail: rinoro@mot.upv.es, Tel: +34 963 877 650 Fax: +34

963 877 659

ABSTRACT

An analysis of in-cylinder gas density and oxygen mass concentration (Y_{O_2}) impact on the mixing and oxidation processes and the final soot emissions in conventional high temperature diffusive Diesel combustion conditions is presented in this paper.

Parametrical tests were performed on a single cylinder heavy-duty research engine. The density was modified adjusting the boost pressure following two approaches, maintaining the Y_{O_2} either before or after the combustion process. The Y_{O_2} was modified by diluting fresh air with exhaust gas maintaining a constant density. The possibility of controlling the soot emissions combining both parameters (Y_{O_2} and density) is evaluated and, in a final part, the NO_x emission results are also addressed.

Results show that Y_{O_2} has a strong effect on both mixing and oxidation processes while density affects principally the mixing process. Both parameters affect the final soot emissions. The density modification through adjustment of boost pressure modifies the trapped mass and has a strong impact on the evolution of Y_{O_2} (thus on the evolution of the mixing process) during combustion. If the density is increased maintaining constant the Y_{O_2} at the beginning of the combustion, the NO_x -Soot trade-off is enhanced.

KEYWORDS: Diesel combustion, mixing process, oxidation process, soot emissions, density, oxygen concentration

DEFINITIONS, ACRONYMS, ABBREVIATIONS

Latin

aTDC	after Top Dead Center
BP	Boost Pressure
CAD	Crank Angle Degree
CO	Carbon monoxide
CO ₂	Carbon dioxide
EGR	Exhaust Gas Recirculation
EOI	End of Injection
FSN	Filter Smoke Number
HC	Unburned Hydrocarbon
HCCI	Homogenous Charge Compression Ignition
HD	Heavy Duty
LTC	Low Temperature Combustion
NO _x	Nitrous Oxides
O ₂	Oxygen
OH	Hydroxyl radicals
PCCI	Premixed Combustion Compression Ignition
PM	Particulate Matter
RoHR	Rate of Heat Release
SOI	Start of Injection
SOC	Start of Combustion
T _{int}	Intake Temperature
T _{flame}	Adiabatic Flame Temperature
T _{ub}	Unburned Gas Temperature
YO ₂	Oxygen mass concentration
YO ₂ -EOC	Oxygen Mass Concentration after the End of Combustion
YO ₂ -SOC	Oxygen Mass Concentration before the Start of Combustion

Greek

ρ	Density
--------	---------

1. INTRODUCTION

Due to its high thermal efficiency and operating economy as well as high torque at low engine speed compared with the spark ignition engine concept, the direct injection Diesel engine is the most widely applied power plant in transportation applications, especially for medium and heavy duty (HD) vehicles.

However, important drawbacks arise with the conventional mixing controlled Diesel combustion, converting it in an important pollutant source for both nitrous oxides (NO_x) and soot emissions (in the present paper soot will be considered as a suitable particulate matter (PM) tracer).¹ Both pollutants are dangerous for human health and also for the environment, leading many world governments to impose increasingly stringent exhaust emissions limits.

In recent years, new combustion concepts aroused with high degree of premixing and low oxygen concentration (YO_2) in order to reduce both NO_x and soot emissions at the same time. However those new concept known as premixed combustion compression ignition (PCCI), homogeneous combustion compression ignition (HCCI) or low temperature combustion (LTC) are usually limited to low load operation due to combustion roughness induce by the high degree of premixing and/or by the limitation of the turbocharger to provide extremely high exhaust gas recirculation (EGR) rate to reduce combustion temperatures at higher loads. Thus, the diffusion controlled combustion is still the most applied combustion strategy at mid and high load in Diesel engines.

In diffusive combustion conditions, the mechanisms involved in the formation/destruction processes and resulting NO_x emissions are basically chemical and are well known. The strategies used to control them are based on acting directly on the chemical kinetic principally by reducing the combustion temperature by lowering YO_2 by means of (cooled) EGR.

Regarding soot emissions, the formation/oxidation mechanisms for a free jet in stationary conditions are also known. They are described for instance in the Dec model²:

- Formation occurs inside the flame. First, at the location of the lift-off and depending on the equivalence ratio at that point, precursors are formed by fuel pyrolysis. Afterwards,

precursors evolve into nuclei before a third process named surface growth during which soot particles accept gas-phase hydrocarbons and see their mass increasing largely.

- Oxidation of the soot formed occurs in the periphery of the flame, where both high temperature and oxygen are available. The exact mechanism of soot oxidation is not well known, however the attack by hydroxyl radicals (OH) is thought to be a major mechanism in near stoichiometric conditions as it is the case in a diffusion flame.^{3,4}

In a free jet in steady conditions the two processes (formation and oxidation) are balanced, the soot formed inside the jet core being oxidized when crossing the flame surface⁵ so that the mass of soot inside the flame remains more or less constant. It is believed that this is also the case for a Diesel flame in a finite space as it is the case for an engine during the quasi-steady process when injection and combustion are overlapped.

However, after the end of injection (EOI), the reactive jet enters in a transitive stage known as the late diffusive combustion. During this stage, the structure of the jet evolves to be completely surrounded by the flame (the lift-off disappears) and the balance between formation and oxidation is affected. On the one hand, the formation process is reduced or even stopped due to the disappearance of rich zone at lift-off location required for soot precursor formation. On the other hand, soot oxidation process is weakened due principally to the diminution of the flame temperature induced by the expansion process. The sooty products previously formed but not oxidized are still inside the volume surrounded by the flame and cannot escape without being oxidized. However, later in the cycle the soot can survive the combustion process through two possible pathways: the exhaust valve opens and there is no sufficient time to complete the burnout, or portions of the flame or reactions around the perimeter become extinguished.⁶

From this very fast description of the soot processes, it appears that in high temperature diffusive combustion conditions it is not soot formation but late soot oxidation that controls final soot emissions. Furthermore, two aspects seem important for late soot oxidation: the time spent to complete the

combustion and the intensity of the oxidation reaction. Indeed if the duration of the late burnt-out is short enough, the flame will not be extinguished or the exhaust valve will not open before the combustion is completed. On the other hand, if the intensity of the oxidation reaction is maintained high enough the reactions around the perimeter of the sooty products pockets will be sustained longer before becoming extinguished.

Two major factors are hence affecting the late soot oxidation:

- The mixing rate, determined by physical processes
- The oxidation rate, determined by chemical processes

These two factors can be affected by injection settings but also by the control of the thermo-chemical conditions of ambient gas in the cylinder.

2. OBJECTIVES AND METHODOLOGY

The study proposed in this paper is focused on the analysis of the in-cylinder gas conditions (density and oxygen concentration) influence on the mixing (physical process) and oxidation (chemical process) rates and finally on the late soot oxidation process, trying to understand the relative importance of the two processes.

All the injection settings have been maintained constant along the study (injection timing, fuel mass injected and injection pressure). Also, the compression ratio and the intake temperature have been maintained constant so the in-cylinder temperature at the beginning of the combustion process was similar in all cases. Tests were performed at mid-load and low speed, engine operation parameters that have been kept constant along the study are presented in the following table 1.

The modification of gas density was performed through the modification of the boost pressure (BP) while the modification of the Y_{O_2} was performed adjusting the EGR rate. The methodology used along the study follows a parametrical scheme varying the density and the Y_{O_2} independently in order to understand isolated effects as well as combined effects of the two parameters.

Compared to infinite volume test rigs, controlling these two parameters in an engine is more complicated since the thermodynamic conditions of the gas are linked between one another and evolve with the time, it is thus necessary to set the experiments taking into account these aspects.

For instance, the density evolves along the combustion due to the piston movement, however since the engine speed and compression ratio have been kept constant the differences in term of density from one case to another will be qualitatively kept along the whole combustion process considering a particular instant of time or crank angle.

On the other hand, this consideration is not valid for the YO_2 . During the combustion, YO_2 diminishes as fuel is burned, and since the fuel mass injected has been maintained constant for all cases the *mass* of oxygen that is consumed during combustion is the same in all cases (considering that combustion efficiency is the same). When varying the density by increasing the boost pressure as it was done in this study, the in-cylinder trapped mass changes and a similar reduction in oxygen *mass* does not result in a similar reduction in oxygen *concentration*. Hence, when studying the influence of the density on late oxidation process maintaining a constant YO_2 , a decision has to be taken on the instant at which the YO_2 is kept constant.

Taking into account the previous considerations, the experiments have been set as follows. In the study of the influence of the YO_2 , the EGR rate was varied maintaining a constant BP. As shown in table 2, the study was performed at two density conditions. The density level corresponds to that of the EOI as this instant marks the beginning of the late diffusive stage of the combustion. Note that, since the density is kept constant for each set of tests, an increase in YO_2 before the start of combustion (YO_2 -SOC) results in an increase in YO_2 after the end of combustion (YO_2 -EOC).

In the study of the influence of the density on the late soot oxidation at constant YO_2 , in a first step, the YO_2 level was kept constant at the beginning of the combustion. As it is shown in table 3, this results in an increase of YO_2 -EOC as the density is increased since the impact of oxygen consumption during combustion is reduced as the in-cylinder trapped mass is increased. Note that in order to maintain

constant the YO_2 -SOC, the EGR rate had to be adapted as the BP was modified. The study was performed at two YO_2 -SOC levels.

In a second step the density was varied maintaining a constant YO_2 -EOC. The settings used for this study are presented in table 4. Once again, the study was performed at two levels of YO_2 -EOC.

The analysis of the late oxidation process and final soot emissions will be hence developed in three parts. First, the analysis of the influence of YO_2 and, second, an analysis of the effect of density that is divided in two parts. A first approach in which the density is varied maintaining YO_2 -SOC and a second approach in which the density is varied maintaining YO_2 -EOC.

The possibility of controlling the soot emissions combining both parameters (YO_2 and density) will be evaluated. Finally, NO_x emissions results will also be addressed in order to identify the actions that can be taken in an engine to optimize the NO_x -Soot trade-off.

3. EXPERIMENTAL SETUP

The engine used in this research is a single-cylinder, four-stroke, direct-injection Diesel research engine since this type of facility generates more accurate data compared to multi-cylinder engines.⁷ In this case, the research engine has 1.8 liters displacement, which is representative of medium-large truck engines. Basic specifications of the engine are included in table 5.

The fuel used in this study is a conventional European Diesel fuel which main specifications are listed in table 6.

The engine was installed in a fully instrumented test cell, with all the auxiliary facilities required for its operation and control as it is illustrated in the scheme presented in figure 1. To achieve stable intake air conditions, a screw compressor supplied the required boost pressure before passing through an air dryer. The air pressure was adjusted within the intake settling chamber while intake temperature was controlled in the intake manifold after mixing with EGR. The exhaust backpressure produced by the

turbine in the real engine was replicated by means of a valve placed in the exhaust system, controlling the pressure in the exhaust settling chamber.

EGR was produced taking exhaust gas from the exhaust settling chamber before passing through a cooler to a settling chamber equipped with an electric heater. It was then introduced into the intake pipe closing the high pressure EGR loop. The temperature regulation was performed upon the EGR-fresh air mixture by means of a temperature sensor in the intake manifold. In order to ensure the required external EGR mass flow rate, the exhaust pressure was maintained at 0.03 MPa above the intake pressure. The exact EGR rate was controlled by means of a valve between the EGR settling chamber and the intake pipe.

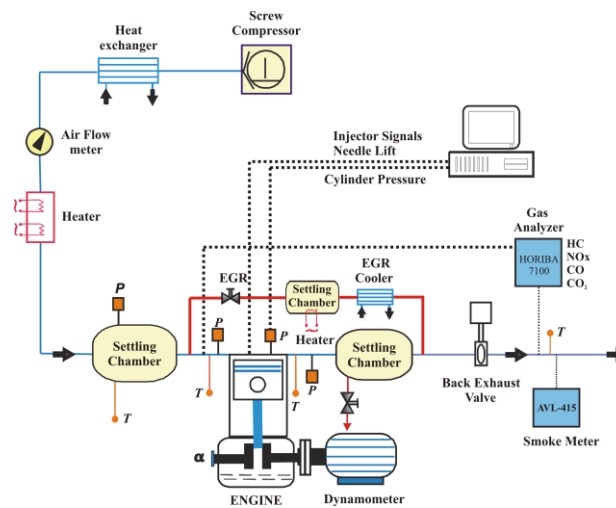


Figure 1. Complete test cell scheme

Concentrations of NO_x , CO, HC, intake and exhaust CO_2 , and O_2 were measured with specific state-of-the-art analyzers. The EGR rate was determined using this experimental measurement of intake and exhaust CO_2 concentrations. Smoke emission was measured with a variable sampling smoke meter, providing results directly in FSN (Filter Smoke Number), units that were transformed into dry soot mass emissions by means of the correlation proposed by Christian et al.⁸ Although the measurement provided do not entirely take into account the soluble organic fraction of the total PM, this measurement has been

shown to give reliable trends.⁹ The fuel injection rate was measured in a commercial test rig following the Bosch system.¹⁰

At each engine operation point, the in-cylinder pressure traces from a piezo-electric transducer were recorded during 50 consecutive engine cycles in order to compensate for dispersion in engine operation. This number of cycles was selected according to the results of a preliminary study.¹¹ Measurements at every operation point were repeated three times and a reference point was controlled before every measuring session to assure tests repeatability along the study.

4. THEORETICAL TOOLS

The recorded traces of in-cylinder pressure were processed by means of a combustion diagnosis code CALMEC.^{12, 13} Valuable information can be extracted, especially the heat release and the rate of heat release (RoHR).

4.1. Characterization of oxidation process intensity:

Oxidation of the soot formed inside the flame takes place outside the flame, principally close to the stoichiometric zone.² The attack by OH-radicals is thought to be a major mechanism in near stoichiometric conditions as it is the case for diffusion flame.^{3, 4}

OH-radicals require the presence of oxygen and high temperature to be formed in large amounts. In a diffusive flame, OH-radicals surround the stoichiometric zone since these two conditions are encountered and impede/limit the soot present inside the flame to escape without being oxidized. The rate of formation of OH-radicals increases exponentially as local temperature increases.^{14, 15, 16}

For the reasons exposed above, in this paper, the faculty of oxidizing soot will be appreciated qualitatively by estimating the instantaneous adiabatic flame temperature (i.e. the maximum local temperature, at the stoichiometric location) along the combustion process.

The adiabatic flame temperature (T_{flame}) is calculated considering a constant pressure at each step of the calculation according to the procedure described in detail in appendix A. 13 species were taken into account in the reaction following the scheme proposed by Way.¹⁷

4.2. Characterization of the mixing rate:

The characteristic mixing time required for a fuel packet injected in a steady state to reach the stoichiometric surface is given in the following the expressions¹⁸:

$$\text{Mixing Time} \propto K_1 \left[(A/F)_{st} \cdot \frac{YO_2 \text{ atm}}{YO_2} \right]^2 \cdot \frac{\emptyset_0}{u_0} \cdot \sqrt{\frac{\rho_f}{\rho}} \quad (1)$$

Where K_1 is a constant that depends on the engine and its configuration, $(A/F)_{st}$ is the stoichiometric air-fuel ratio, $YO_2\text{-atm}$ and YO_2 are respectively the oxygen mass concentration in the atmosphere and in the cylinder, \emptyset_0 is the nozzle orifice diameter, u_0 the injection velocity and finally ρ_f and ρ are respectively the density of the fuel and the density of the gas inside the cylinder.

The mixing process between fuel and oxygen during diffusive combustion depends on different parameters that can be separated in two classes:

- The injection parameters: injection velocity, nozzle hole diameter and geometry, fuel properties and composition
- The in-cylinder gas parameters: density and oxygen concentration

In the present study, the injection parameters were maintained constant so the equation can be re-written as follow:

$$\text{Mixing Time} \propto K_2 \left[YO_2^2 \cdot \rho^{0.5} \right]^{-1} \quad (2)$$

Where:

$$K_2 = K_1 \cdot \left[(A/F)_{st} \cdot YO_2 \text{ atm} \right]^2 \cdot \frac{\emptyset_0}{u_0} \cdot \sqrt{\rho_f} \quad (3)$$

Equation (2) is valid for inert conditions, i.e. when there is no heat released at the stoichiometric location. In reactive condition, the high local temperature in that zone has a negative effect on mixing process.^{18, 19, 20} García²¹ details that this is due to a reduction in local density and propose a correction of the previous equation with a factor $\sqrt{\rho_{mix}/\rho_{comb}}$, where ρ_{mix} is the local (in stoichiometric conditions) density of the mixture fuel/gas in inert conditions and ρ_{comb} the local density of the mixture in reactive conditions. Considering a constant pressure in the combustion chamber this correction factor can be also approximated as the square root of the ratio between T_{flame} and the unburned gas temperature (T_{ub}) as it was also found by other authors.^{22, 23}

The mixing process will be appreciated qualitatively through the mixing capacity of the in-cylinder gas (inverse of the characteristic mixing time) from the final equation given below, in arbitrary units:

$$Gas\ Mixing\ Capacity \propto \frac{1}{Mixing\ Time \cdot \sqrt{\frac{T_{flame}}{T_{ub}}}} \propto [YO_2^2 \cdot \rho^{0.5}] \cdot \sqrt{\frac{T_{ub}}{T_{flame}}} \quad (4)$$

Note that during the ignition delay there is no flame so the factor $\sqrt{\frac{T_{ub}}{T_{flame}}}$ is equal to one.

5. RESULTS

In this section, the combustion and soot emission results are addressed. Firstly, instantaneous results of the overall combustion process will be shown as an overview. Next, the analysis will focus on the mixing and oxidation conditions at the EOI and finally the soot emission results will be discussed. The instant of the EOI was chosen as it marks the beginning of the late diffusive combustion stage which is crucial for the late soot oxidation (and final soot emissions) in high temperature Diesel combustion, as it was previously discussed.

5.1. Influence of oxygen concentration:

The influence of the oxygen concentration on the RoHR, T_{flame} and the gas mixing capacity versus the crank angle is shown in figure 3.

As it can be observed, YO_2 -SOC has little effect on the RoHR, although it is clear that the trend when lowering the oxygen concentration is to reduce RoHR during the injection process.

On the other hand, the effect shown on T_{flame} is strong. As it is widely known, a lower YO_2 -SOC produces lower flame temperature due to the dilution of the oxygen in inert gas. The effect observed on the gas mixing capacity is the same with a reduction predicted as the YO_2 -SOC is reduced. It takes indeed longer for the fuel injected to mix with oxygen when oxygen concentration is reduced since more gas has to be entrained in the spray to reach a stoichiometric mixture.

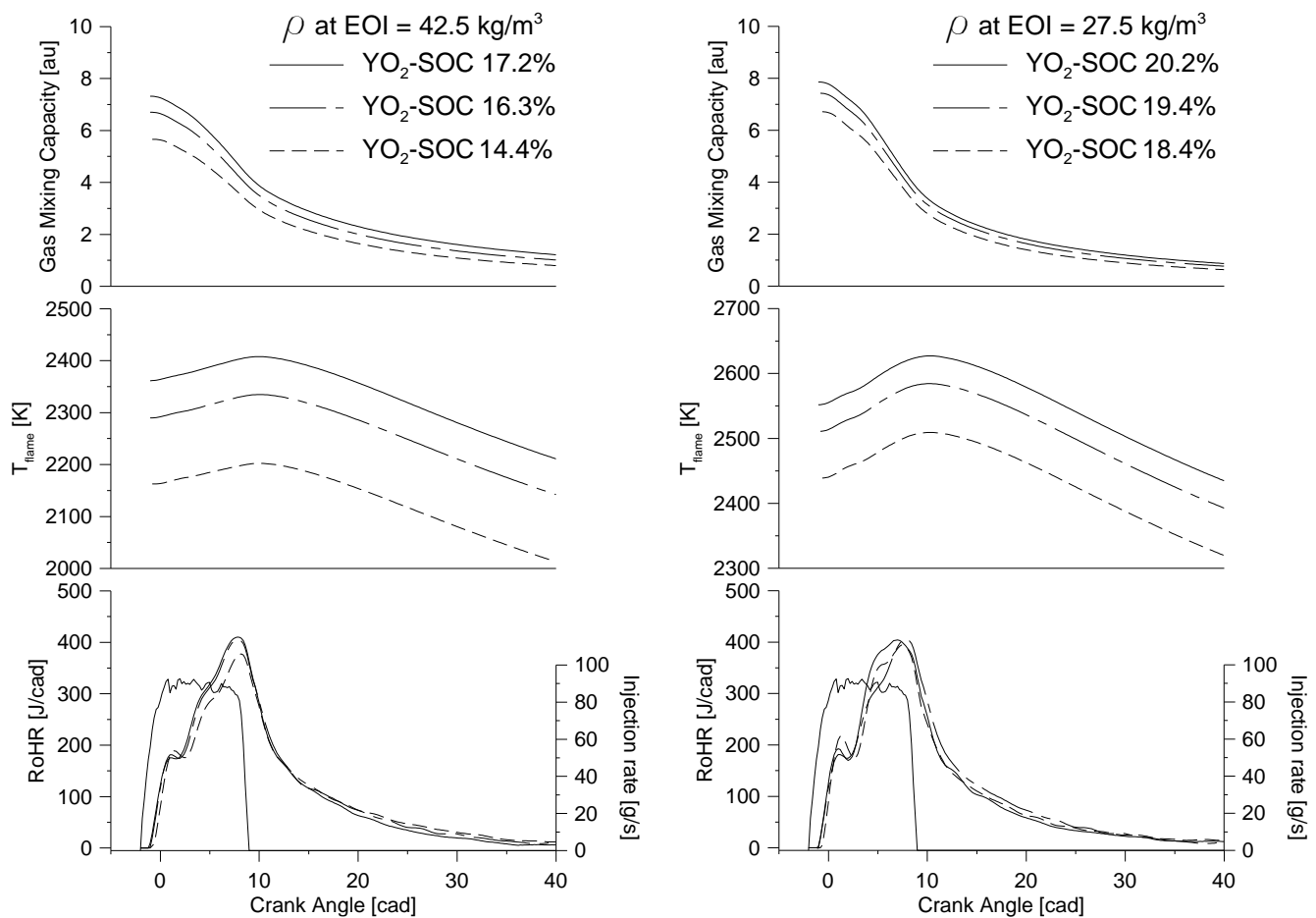


Figure 3. RoHR, T_{flame} and gas mixing capacity evolution along combustion for various YO_2 -SOC maintaining a constant density, for two density levels

Focusing on the conditions at the EOI i.e. at the beginning of the late diffusive stage, it is shown in figure 4 that T_{flame} at the beginning of this stage is almost linearly dependent on the $YO_2\text{-SOC}$ and remains almost unaffected by density. On the other hand, gas mixing capacity is dependent on both parameters. Considering a constant density, the gas mixing capacity is largely improved as $YO_2\text{-SOC}$ increases for the reasons exposed previously.

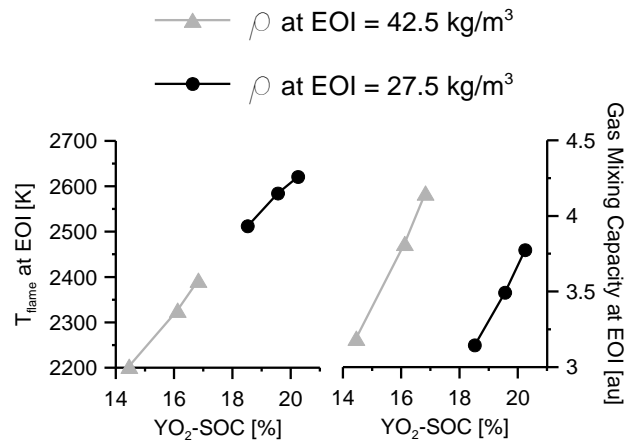


Figure 4. T_{flame} and gas mixing capacity at the EOI when varying $YO_2\text{-SOC}$ maintaining a constant density, for two density levels

Figure 5 shows an experimental result describing the mixing process: the fraction of fuel mass burned at the EOI. The trends observed are in agreement with the gas mixing capacity calculations shown in previous figure 4 for the effect of the $YO_2\text{-SOC}$, however the effect of density seems to be weaker.

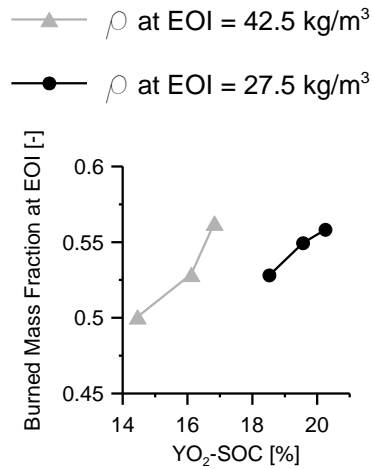


Figure 5. Burned mass fraction at EOI when varying YO₂-SOC maintaining a constant density for two density levels

Two phenomenon can explain this difference. First, the initial part of the mixing occurs (during ignition delay) in inert condition so the high YO₂-SOC cases are less affected by the negative effect of low local density due to heat release at stoichiometric location. Also, during the injection process, no flame is present around the lift-off so equation (4) over-estimates the negative effect of low local density due to high flame temperature during this period.

However, after the EOI, the lift-off disappears and the flame surrounds completely the remaining reactants, so the trends given in figure 4 are likely to be closer to the reality of the intensity of the mixing process during the late diffusive stage than the experimental indicator of the fuel mass burned at the instant of the EOI.

Figure 6 presents the soot emissions results. It is clear that the effect of increasing YO₂-SOC is a reduction of the soot emissions. As commented in the introduction, soot formation is very high in all cases and tendencies in final soot emissions cannot be explained considering the formation process.

Indeed, although it was shown by Idicheria et al.²⁴ that soot formation increases with a reduction of oxygen concentration, the magnitude of the increase is small. Decreasing the volumetric oxygen concentration from 21% down to 15% an increase of 30% in soot formation was measured.²⁴ This

increase in soot formation cannot explain the augmentation by two orders of magnitude observed here in final soot emissions when reducing YO₂-SOC from 17.2% to 14.4% in high density case.

On the other hand this result is easily explained by the late-oxidation. The higher T_{flame} encountered with higher oxygen concentration makes the late oxidation process more effective reducing final soot emissions.

However it can also be observed that soot emissions are affected by the ambient density, as was the gas mixing capacity, while the T_{flame} is not. The importance of the density on final soot emissions will be discussed in the following section.

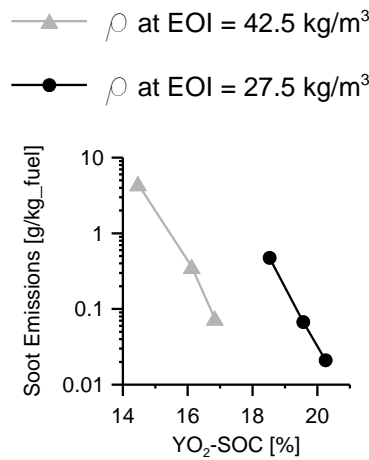


Figure 6. Indicated soot emissions when varying YO₂-SOC maintaining a constant density for two density levels

5.2. Influence of density:

It was commented previously that density was varied following two approaches since the modification was obtained adjusting the trapped mass. It is highlighted in following figure 7 that due to the modified trapped mass, the reduction in YO₂ along the combustion process is different as the density is varied.

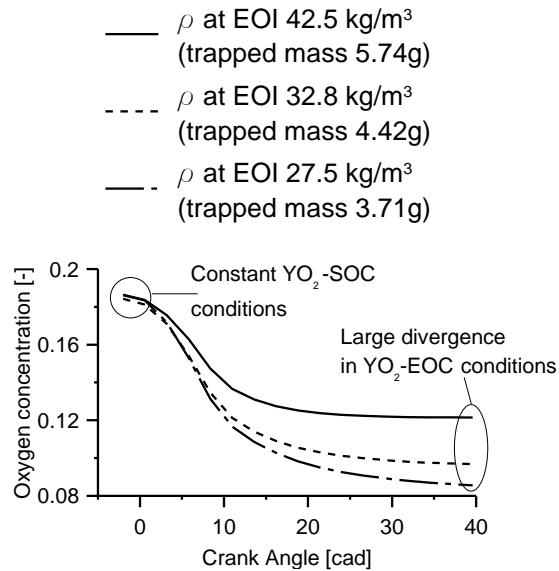


Figure 7. YO_2 evolution along combustion when varying in-cylinder density maintaining a constant YO_2 -SOC level

Given this consideration, the study of the influence of density was performed following two approaches. First the density was modified maintaining a constant oxygen concentration at the beginning of the combustion process while, in a second approach, settings have been adjusted in order to keep the oxygen concentration constant at the end of the combustion process.

5.2.1. Constant YO_2 -SOC results:

The influence of the density variation with constant YO_2 -SOC on the $RoHR$, T_{flame} and the gas mixing capacity versus the crank angle is shown in figure 8.

An increase in the density with constant YO_2 -SOC results in a slight increase of the $RoHR$ during the injection process while the effect on T_{flame} is weak since gas temperature and YO_2 -SOC are maintained constant. A lower density leads to a slight increase in T_{flame} along the combustion process. This is a consequence of the reduced in cylinder mass as density is decreased, implying a higher pressure rise due to combustion. The higher pressure rise has a direct effect on T_{ub} explaining the final increase observed in T_{flame} .

On the other hand the effect of density on mixing process is strong, increased density with constant YO_2 -SOC leading to increased gas mixing capacity as the density appears directly in equation (4). The impact of density modification on gas mixing capacity is observed from the beginning of the combustion process and gets relatively more important as combustion process takes place. This is due to the fact that YO_2 drops more largely during the combustion for low density cases as shown in figure 7, leading to larger drop in gas mixing capacity for those cases since YO_2 also appears in equation (4).

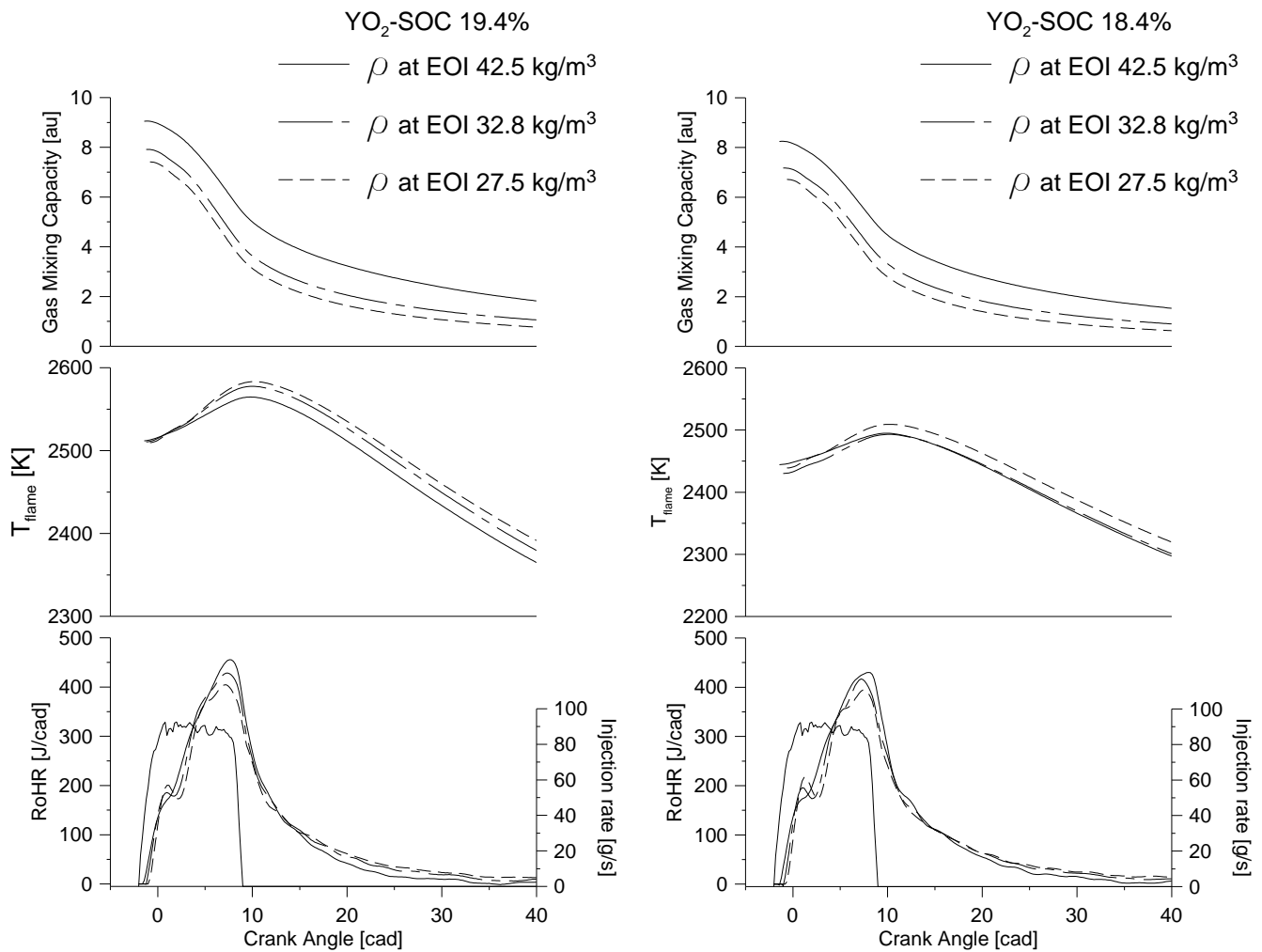


Figure 8. RoHR, T_{flame} and gas mixing capacity evolution along combustion for various densities keeping constant YO_2 -SOC for two YO_2 -SOC levels

Regarding conditions at the beginning of the late combustion stage shown in figure 9, T_{flame} is almost unchanged (slightly reduced as density is increased) however the mixing process is greatly affected by the variation of the density as it was commented previously.

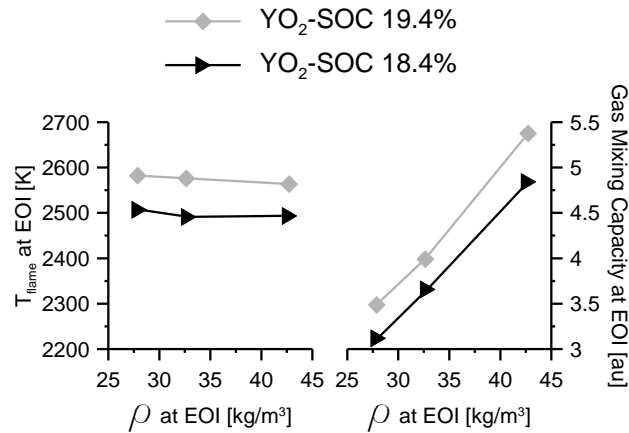


Figure 9. T_{flame} and gas mixing capacity at the EOI when varying density keeping constant YO₂-SOC for two YO₂-SOC levels

Despite that on figure 8 the RoHR did not appear strongly enhanced during the injection as density was increased, the following figure 10 shows that in fact the fuel mass burned at the end of the injection process is much higher as in-cylinder density increases as it was suggested by the trends in the gas mixing capacity.

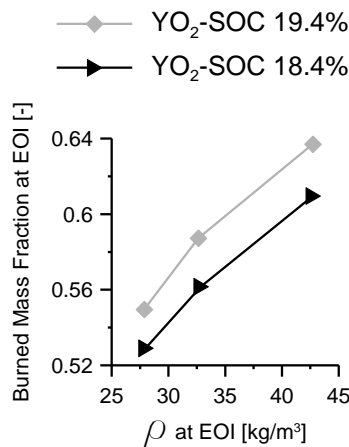


Figure 10. Burned mass fraction at EOI when varying density keeping constant YO₂-SOC for two YO₂-SOC levels

The final soot emissions results are presented in following figure 11. Soot formation is believed to increase with density in the cases presented here for two reasons. First, higher pressure found for higher density cases leads to higher soot formation (at a rate which could be as high as the pressure squared).⁴ On the other hand, density has a double effect on lift-off. It reduces its length and increases the rate of gas entrainment, the net effect being a small decrease in the amount of air entrained at the lift-off length. The final consequence is an increase in equivalence ratio at lift-off leading to higher soot precursors formation.⁴ It is confirmed by Pickett et al.²³ that an increase in ambient gas density for constant ambient gas temperature and oxygen concentration results in a large increase in peak soot volume fraction inside the jet, the dependence observed being proportional to between $\rho^{2.2}$ and $\rho^{2.5}$.

Finally, despite the similar T_{flame} at the beginning of the late combustion stage and the supposed increase in soot formation, figure 11 shows that soot emissions are largely reduced as density is increased, meaning that an enhanced mixing process has a strong importance on late oxidation and final soot emissions.

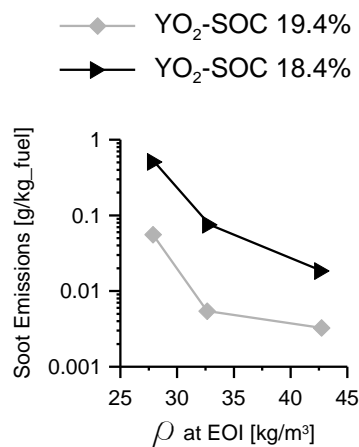


Figure 11. Indicated soot emissions when varying density for two YO₂-SOC levels

In order to highlight the mixing process impact on the oxidation process, the evolution of T_{flame} during the late diffusive combustion stage, i.e. from the EOI to the EOC, is presented in figure 12. Note that the EOC has been defined as the instant when the fraction of fuel mass burned (FMB) reaches 95%.

Higher in-cylinder gas density enhances the mixing process, leading to a reduced combustion duration. This implies that EOC occurs earlier as density increases. As it can be observed in figures 8 and 12, during the late combustion stage, T_{flame} decreases due to expansion process. Because of this, if T_{flame} is similar at the EOI (as it is the case when increasing density maintaining a constant YO_2 -SOC), shorter combustion duration (i.e. earlier EOC) makes that combustion ends with higher T_{flame} . This means that the last fuel pockets containing sooty products finish their burnout surrounded with higher concentration of OH-radicals, the fraction of soot escaping those pockets is thus reduced explaining the final soot emission results shown in figure 11.

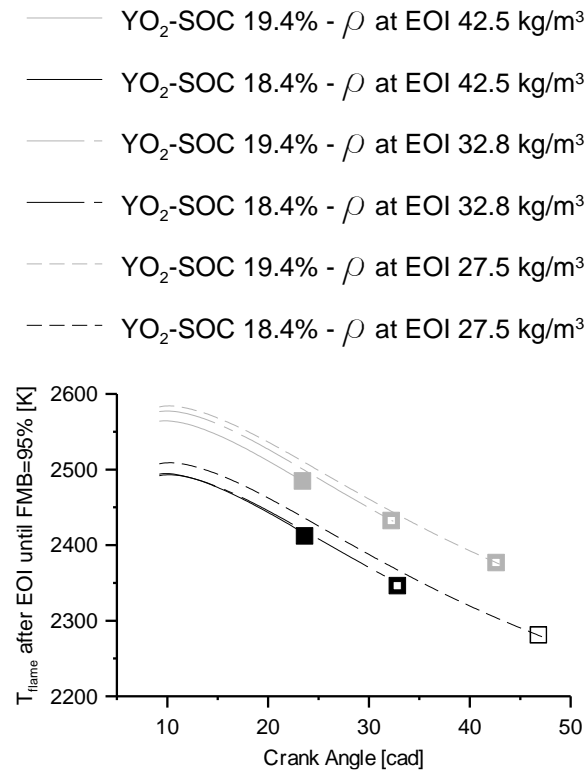


Figure 12. T_{flame} evolution along late diffusive stage when varying in-cylinder density keeping constant $Y_{O_2}\text{-SOC}$ for two $Y_{O_2}\text{-SOC}$ levels

5.2.2. *Constant $Y_{O_2}\text{-EOC}$ results:*

In this second approach, a set of tests varying density keeping $Y_{O_2}\text{-EOC}$ constant is analyzed. In this case the combustion begins with lower oxygen concentration when density is increased.

In figure 13, the instantaneous results of combustion when varying density keeping constant $Y_{O_2}\text{-EOC}$ are displayed.

On the bottom graph it can be observed that RoHR during the injection process is slightly reduced as density is increased. This trend is confirmed by the gas mixing capacity that is lower for high density cases at the beginning of the combustion. This is the result of a competition between increased density and reduced oxygen concentration at the beginning of the combustion process that, for the fuel mass injected considered in the study, leads to higher mixing capacity for low density cases at the beginning of the combustion. As the combustion process takes place, the trend is inverted because of the larger reduction in oxygen concentration for low density cases (see figure 7).

With respect to T_{flame} , the lower oxygen concentration at the beginning of the combustion process for the high density cases leads to lower T_{flame} . T_{flame} is not affected by oxygen concentration evolution along combustion process, thus the differences in this parameter are kept along the whole combustion process.

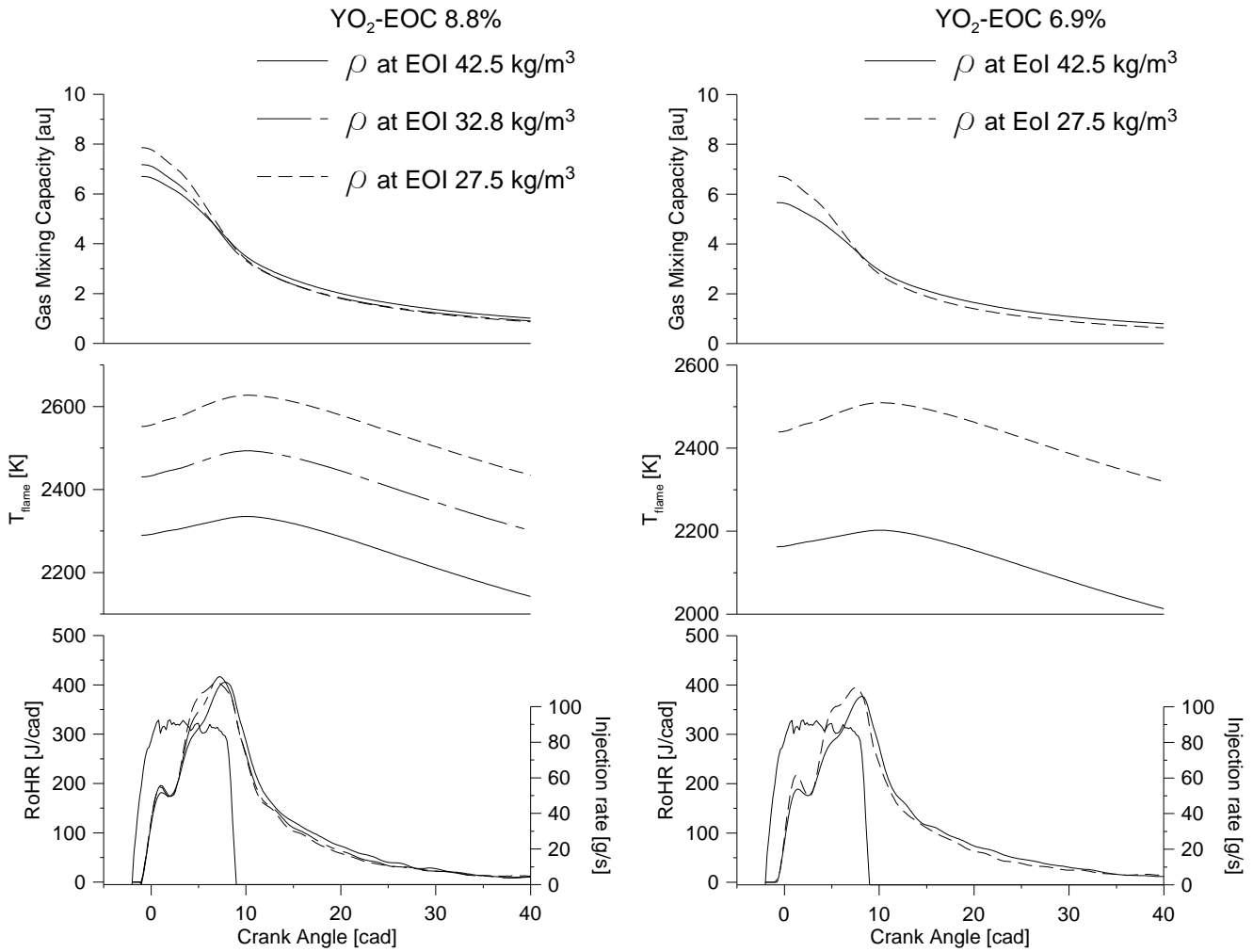


Figure 13. RoHR, T_{flame} and gas mixing capacity evolution along combustion for various densities keeping constant $\text{YO}_2\text{-EOC}$ for two $\text{YO}_2\text{-EOC}$ levels

Regarding indicators at the EOI shown in figure 14, T_{flame} follows the trends described previously i.e. increasing density leads to a reduced T_{flame} . On the other hand, gas mixing capacity that was higher at the beginning of the combustion process for low density cases, results to be approximately constant at the beginning of the late combustion stage for the different density levels.

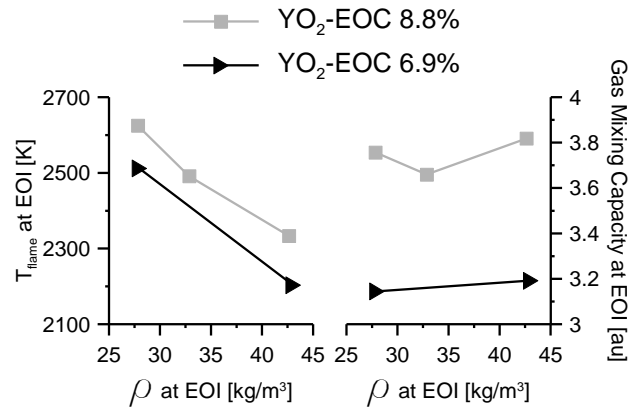


Figure 14. T_{flame} and gas mixing capacity at the EOI when varying density maintaining a constant YO₂-EOC for two YO₂-EOC levels

This combination of parameters leads to higher soot emissions as density is increased (see figure 15). Again the final result in soot emissions can be explained through oxidation trends: the clear reduction observed in T_{flame} as density is increased implies weaker oxidation process while the similar mixing capacity at the EOI results in equivalent late combustion stage duration.

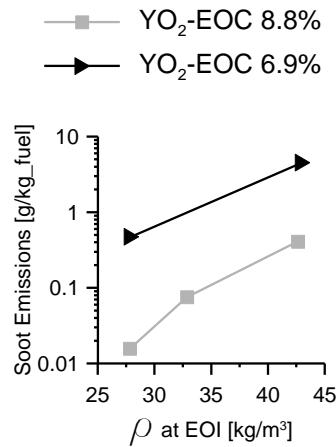


Figure 15. Indicated soot emissions when varying density maintaining constant YO₂-EOC for two YO₂-EOC levels

The evolution of T_{flame} during the late diffusive combustion is shown in figure 16 for the three cases with $Y_{O_2}\text{-EOC}$ set at 8.8%. The trends exposed previously are highlighted in that figure. As density is increased, late diffusive stage starts with a lower T_{flame} and the duration of the late diffusive stage is then weakly affected since higher density and lower oxygen concentration affect mixing process in opposite ways. The slightly longer late diffusive combustion process in case of low density is due to the fact that as combustion takes place, the difference in Y_{O_2} disappears leading to worsened mixing process. Finally as density is increased, and despite the slightly shorter late diffusive stage duration, the combustion ends with a lower T_{flame} explaining the increase in soot emissions shown in figure 15..

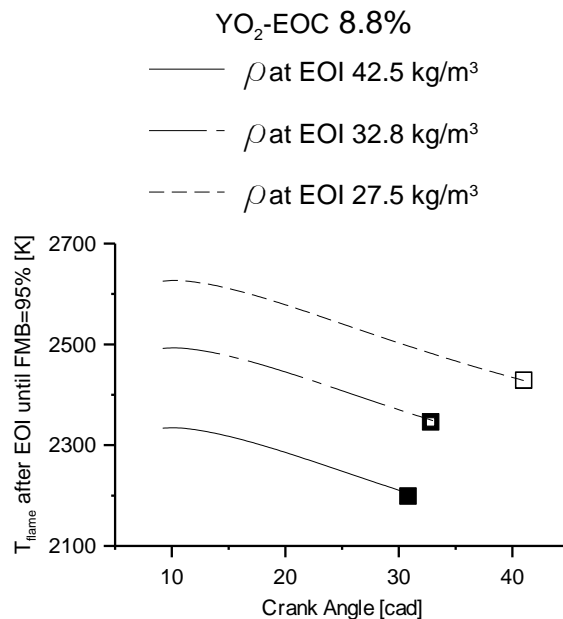


Figure 16. T_{flame} evolution along the late diffusive stage when varying in-cylinder density for a constant $Y_{O_2}\text{-EOC}$ for two $Y_{O_2}\text{-EOC}$ levels

5.3. Global evaluation of the NO_x and soot emissions combination and control

Regarding the impact of density, in a first approach it was shown that increasing density maintaining a constant $Y_{O_2}\text{-SOC}$ permitted a large reduction in soot emission due to a similar T_{flame} and shorter combustion duration. In a second approach the density was varied maintaining a constant $Y_{O_2}\text{-EOC}$; in

that case soot emissions were found to increase with an increase in density due to a large reduction in T_{flame} . It seems so that the first approach (to vary density maintaining constant Y_{O_2-SOC}) is a much better option for soot emissions control compared to the second one. However to gain a more global view on engine emissions performance, NO_x emissions, that are known to be highly dependent on maximum T_{flame} during the combustion process,³ should also be observed.

In the following figure 17, the evolution of T_{flame} during the combustion process (from SOC to FMB=95%) is plotted for the cases discussed previously, varying the density for constant Y_{O_2-SOC} . The maximum T_{flame} found during the combustion and T_{flame} at the EOC are highlighted with symbols on the graph.

It is observable that for a constant Y_{O_2-SOC} , the maximum T_{flame} remains more or less constant while the temperature at the end of the combustion is higher as the density is increased. In this same figure 17, the indicated NO_x and soot emission results are displayed. It can be observed that, as the maximum T_{flame} is almost not affected by the density for a constant Y_{O_2-SOC} , the indicated NO_x emissions remain approximately unaffected by an increase in density while, on the other hand, soot emissions are largely reduced due to higher T_{flame} at EOC.

It is interesting to note that an increase in density with a constant Y_{O_2-SOC} permits in fact to enhance the NO_x -Soot trade-off with reduced soot emissions for constant NO_x emissions.

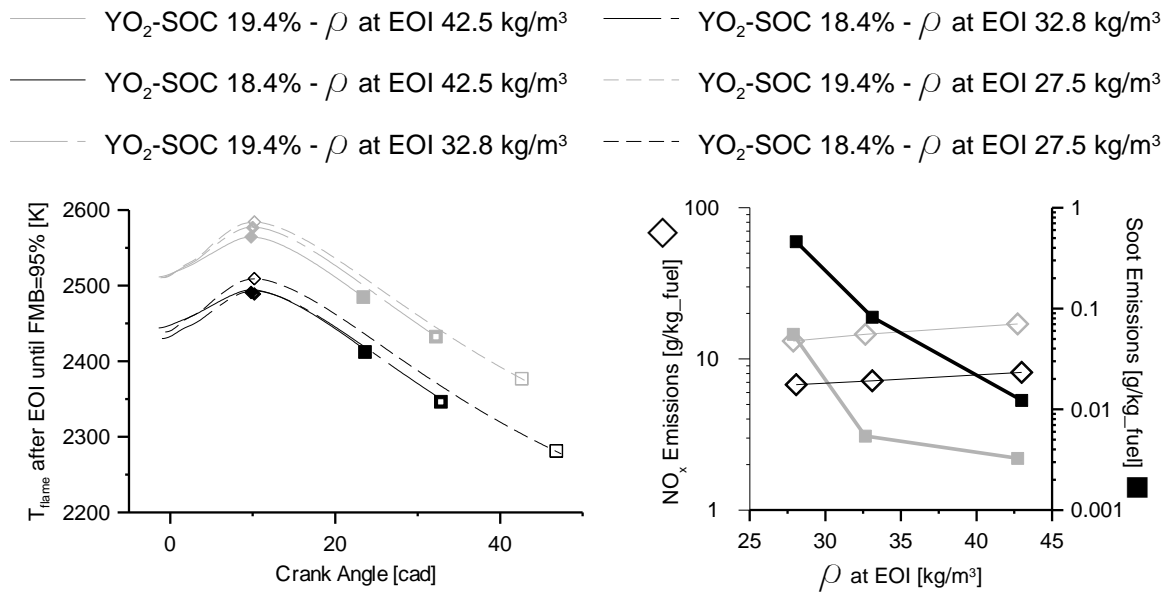


Figure 17. Left. T_{flame} evolution along the combustion when varying in-cylinder density for a constant YO₂-SOC level. **Right.** Indicated NO_x (diamonds symbols) and soot (squared symbols) emissions corresponding to the cases shown on the left graph.

Considering now the second set of tests in which density was varied maintaining a constant YO₂-EOC, the evolution of T_{flame} during the combustion process is shown in figure 18 with the maximum and final T_{flame} highlighted with symbols. On the right part of the figure, the corresponding NO_x and soot emissions in indicative values are shown.

In this case, soot emissions increase as the density is increased due to the lower T_{flame} at the EOC. However NO_x emissions are largely reduced since the maximal T_{flame} reached during the combustion is much lower in the high density cases.

In spite that this second approach is not interesting in terms of soot emissions compared to the first one, NO_x emissions are shown to be largely reduced as density is increased while they were maintained constant in the first approach.

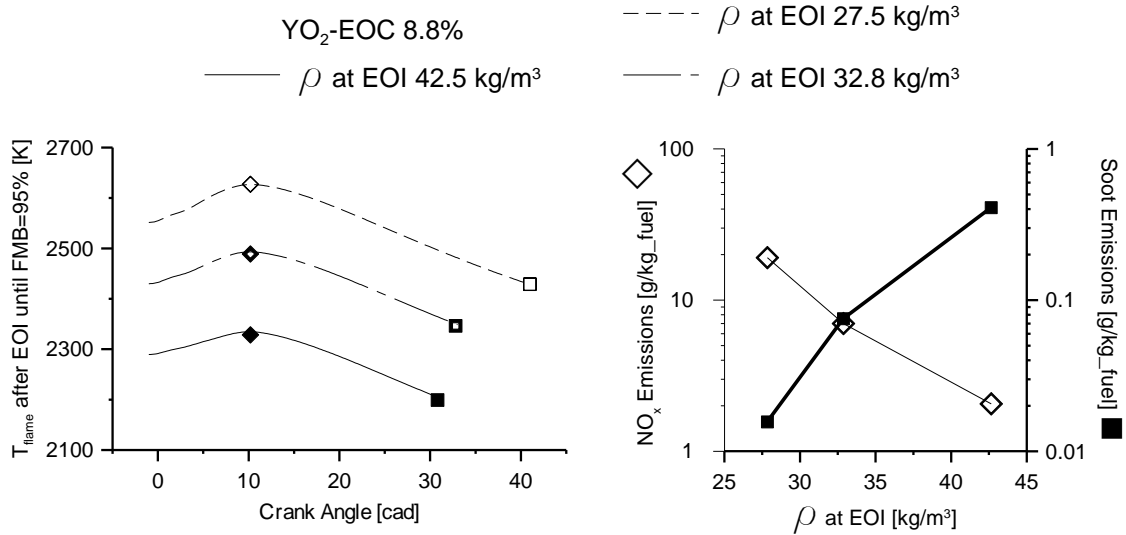


Figure 18. Left. T_{flame} evolution along the combustion when varying in-cylinder density for a constant $\text{YO}_2\text{-EOC}$ level. **Right.** Indicated NO_x (diamonds symbols) and soot emissions (squared symbols) corresponding to the cases shown on the left graph.

6. CONCLUSIONS

A study has been performed on the effect of in-cylinder gas density and oxygen concentration on mixing and oxidation processes in high-temperature Diesel combustion. The main conclusions of the study are the following:

- Increasing $\text{YO}_2\text{-SOC}$ maintaining a constant density leads to both enhanced mixing and oxidation processes explaining why final soot emissions are largely reduced in that case
- An increase in density with constant $\text{YO}_2\text{-SOC}$ leads to enhanced mixing process while oxidation intensity is not affected. Final soot emissions are largely reduced because reduced combustion duration (due to enhanced mixing process) permits a limited drop in T_{flame} during the late combustion stage i.e. combustion ends with a higher T_{flame}
- Maximum T_{flame} is almost unaffected by density increase at constant $\text{YO}_2\text{-SOC}$ so that NO_x emissions remain approximately constant while soot emissions are largely reduced. Increased

density maintaining a constant YO_2 -SOC appears so to be option to enhance to NO_x -Soot trade-off in high temperature diffusive Diesel combustion conditions

- An increase in density maintaining a constant YO_2 -EOC implies that YO_2 -SOC is reduced. The effect on the mixing process during the first stages of the combustion is then the result of a competition between higher density (that tends to enhance mixing process) and lower YO_2 (that tends to worsen mixing process). For the fuel mass injected considered in the study (that is representative of mid-load operation point) the balance turns out to slow down the mixing process during the first stages of the combustion as density is increased. However the trend is inverted as the combustion takes place.
- Increased density maintaining a constant YO_2 -EOC leads to lower T_{flame} as the YO_2 -SOC is reduced. At the EOC, even though the late diffusive stage duration is slightly shorter as density is increased, T_{flame} remains much lower leading to higher soot emissions. On the other hand, the lower T_{flame} during the combustion process permits a large reduction in NO_x emissions

7. REFERENCES

1. Kittelson, D.B.; Arnold, M.; Watts W.F. *Review of diesel particulate matter sampling methods. Final report*; Prepared by the University of Minnesota for the U.S. Environmental Protection Agency, 1999.
2. Dec, J.E. *SAE Trans.* **1997**, *106*, 1319–1348.
3. Heywood, J.B. *Internal Combustion Engine Fundamentals*; McGraw-Hill, 1988.
4. Tree, D.R.; Svensson, K.I.. *Prog. Energ. Combust.* **2007**, *33*, 272-309.
5. Flynn, P.F.; Durrett, R.P.; Hunter, G.L.; Loye, A.O.; Akinyemi, O.C.; Dec, J.E.; Westbrook, C.K. *SAE Paper.* **1999**, 1999-01-0509.
6. Dec, J.E.; Kelly-Zion, L. *SAE Paper.* **2000**, 2000-01-0238.

7. Benajes, J.; López, J.J.; Novella, R.; García, A. *Exp. Techniques*. **2008**, *32*, 41-47.
8. Christian, R.; Knopf, F.; Jasmek, A.; Schindler, W.A. *MTZ*. **1993**, *54*, 16-22.
9. Kolodziej, C.; Wirojsakunchai, E.; Foster, D.E.; Schmidt, N.; Kamimoto, T.; Kawai, T.; Akard, M.; Yoshimura, T. *SAE paper*. **2007**, 2007-01-1945.
10. Bosch, W. *SAE Paper*. **1966**, 660749.
11. Lancaster, D.R.; Krieger, R.B. Lienesch, J.H. *SAE Paper*. **1975**, 750026.
12. Lapuerta, M.; Armas, O.; Hernández, J.J. *Appl. Therm. Eng.* **1999**, *19*, 513–529.
13. Payri, F.; Molina, S.; Martín, J.; Armas, O. *Appl. Therm. Eng.* **2006**, *26*, 226–236.
14. Bergman, M.; Golovitchev, V. I. *SAE Paper*. **2007**, 2007-01-1086.
15. Fujimoto, H.; Kurata, K.; Asai, G.; Senda, J. *SAE Paper*. **1998**, 982630.
16. Fenimore, C.P.; Jones, G.W. *J. Phys. Chem.* **1967**, *3*, 71.
17. Way, R.J.B. *P. I. Mech. Eng.* **1976**, *190*, 686-697.
18. Arrègle, J.; López, J.J.; García, J.M. ; Fenellosa, C. *Appl. Therm. Eng.* **2003**, *23*, 1301–1317.
19. Han, D.; Mungal, M.G. *Combust. Flame*. **2001**, *124*, 370–386.
20. Arrègle, J.; López, J.J.; Martín, J.; Mocholí, E.M. *SAE Paper*. **2006**, 2006-01-1382.
21. García, J.M. Doctoral Thesis, Universidad Politécnica de Valencia, Departamento de Máquinas y Motores Térmicos (in spanish), 2004.
22. Becker, H.A.; Liang, D. *Combust. Flame*. **1978**, *32*, 115–137.
23. Pickett, L.M.; Siebers, D.L. *Combust. Flame*. **2004**, *138*, 114–135.
24. Idicheria, C.A.; Pickett, L.M. *SAE Paper*. **2005**, 2005-01-3834.

APPENDIX A: Calculation of the adiabatic flame temperature

The adiabatic flame temperature has been calculated assuming the three main hypotheses listed below, which are widely accepted by the Diesel combustion research community:

- The combustion is considered to take place at constant pressure at each time step.
- The fuel/air mixture burns adiabatically, which implies that all the heat released during combustion is used to increase the temperature of the combustion products.
- A conventional chemical equilibrium model taking into account the dissociation phenomena is assumed.

Considering these assumptions, the absolute enthalpy of the reactants at the initial state equals the absolute enthalpy of the products at the final state. This statement is expressed in the next equation (A.1):

$$H_{initial}(P, T_{ub}) = H_{final}(P, T_{flame}) \quad (A.1)$$

In this equation, P represents the instantaneous in-cylinder pressure and it is directly measured in the research engine, T_{flame} is the desired output variable and T_{ub} means the temperature of the unburned gases.

In this calculation scheme, T_{ub} acts as an input and it should be obtained before computing T_{flame} . It is worthy to note that the temperature of the unburned gases and the in-cylinder mean temperature are the same until the start of combustion. Once the combustion process starts, the unburned gases are assumed to undergo a sequence of adiabatic compression processes each time step according to measured in-cylinder pressure profile. This idea is reflected in the following equation (A.2).

$$T_{ub\ i}(\alpha) = T_{ub\ i-1}(\alpha) \cdot \left(\frac{P_i}{P_{i-1}} \right)^{\frac{\gamma-1}{\gamma}} \quad (A.2)$$

Where:

P_i : is the in-cylinder pressure at the i^{th} instant.

$T_{ub,i}$: is the unburned gases temperature at the i^{th} instant.

P_{i-1} : is the in-cylinder pressure at the $(i-1)^{\text{th}}$ instant

$T_{ub,i-1}$: is the unburned gases temperature at the $(i-1)^{\text{th}}$ instant.

γ : is the ratio of specific heats.

According to the equation (A.2), the unburned gases temperature at a given instant ($T_{ub,i}$) is calculated from that of the previous instant one time step before ($T_{ub,i-1}$). This algorithm starts together with the combustion process and therefore, the initial $T_{ub,0}$ and $P_{ub,0}$ correspond with the mean in-cylinder temperature and pressure at the start of combustion directly provided by the combustion diagnosis code.

Once the computation of T_{ub} is explained, the adiabatic flame temperature can be computed from equation (A.1). In order to compute the enthalpies at both the initial and final states of the combustion process (i.e. the enthalpy of the reactants and the combustion products), the initial and final composition of the gases has to be known.

Regarding the details of the thermodynamic calculations, the enthalpy for a mixture of elements can be expressed as:

$$H_{mixture}(T) = \sum_{i=1}^N N_i \cdot H_i(T) \quad (A.3)$$

$$H_i = h_{i,form} + \int_{T=298.15}^T C_{p_i} dT \quad (A.4)$$

Where

- $H_{mixture}$: is the total enthalpy of the mixture, which depends on its temperature and composition.

- H_i : is the enthalpy of each individual element of the mixture.
- $h_{i,\text{form}}$: is the formation enthalpy for each element (computed at standard conditions: 298.15 K and 1 bar). These values are available in thermodynamic data bases.
- N_i : is the moles number of each element of the mixture.
- C_{pi} : is the heat capacity at constant pressure for each element of the mixture, available in thermodynamic data bases as a polynomial expression in terms of temperature, and
- N : is the number of chemical elements in the mixture.

The unburned gases composition is known, whereas the combustion products composition depends on their final temperature, i.e. the adiabatic flame temperature. Because of this link between products composition and temperature, the computation of the adiabatic flame temperature becomes an iterative process.

TABLES

Table1: Constant engine operation parameters along the study

Speed [rpm]	Load [%]	Fuel mass [mg/st]	Injection Pressure [bar]	SoI [cad aTDC]	T _{int} [°C]
1200	50	117	1950	-4	51

Table 2. Test matrix for the study of the influence of YO₂ maintaining a constant density (for two density levels)

ρ at EOI [kg/m ³]	BP [bar]	YO ₂ -SOC [%]	EGR [%]	YO ₂ -EOC [%]
27.5	2	20.2	20.5	8.8
		19.4	24	7.9
		18.4	29	6.9
42.5	3	17.2	45	9.7
		16.3	48	8.8
		14.4	54	6.9

Table 3. Test matrix for the study of the influence of density maintaining a constant YO₂-SOC (for two YO₂-SOC levels)

ρ at EOI [kg/m ³]	BP [bar]	YO ₂ -SOC [%]	EGR [%]	YO ₂ -EOC [%]
27.5	2	19.4	24	7.9
32.8	2.3		28	9.7
42.5	3		33	12
27.5	2	18.4	29	6.9
32.8	2.3		33	8.8
42.5	3		45	11

Table 4. Test matrix for the study of the influence of density maintaining a constant YO₂-EOC (for two YO₂-EOC levels)

ρ at EOI [kg/m ³]	BP [bar]	YO ₂ -SOC [%]	EGR [%]	YO ₂ -EOC [%]
27.5	2	18.4	29	6.9
42.5	3	14.4	54	
27.5	2	20.2	20.5	8.8
32.8	2.3	18.4	33	
42.5	3	16.3	48	

Table 5. Main research engine characteristics

Engine Type	Direct-injection Diesel, 4 Stroke-cycle single cylinder
Bore x Stroke	123 x 152 mm
Displacement	1.8 dm ³
Compression Ratio	16.3
Fuel Injection System	Common-rail + Pressure amplifier piston. Solenoid system
Injection Nozzle	6 holes x 0.214 mm
Spray included angle	140°

Table 6. Diesel fuel main characteristics

Test	Units	Results
Cetane number	---	51,52
Density @ 15°C	kg/m ³	843,0
Sulphur content	mg/kg	27,9
Distillation	---	--
65%	°C	294,5

85%	°C	329,2
95%	°C	357,0
Viscosity @ 40°C	mm ² /s	2,847
Upper Heating Value	Kc/Kg.	10905
Lower Heating Value	Kc/Kg.	10236